Nonlinear oscillations and chaotic response of Shape Memory Alloys

Mohamed Ould Moussa[1], Ziad Moumni[1], Olivier Doaré[1], Cyril Touzé[1], and Wael Zaki[2]

[1]Unité de Mécanique (UME), ENSTA-ParisTech, Chemin de la Hunière, 91761 Palaiseau Cedex, France
[2]Khalifa University of Science, Technology and Research (KUSTAR), PO.Box 127788, Abu Dhabi, UAE
(E-mail: `mohamed.ould-moussa@polytechnique.edu`)

Abstract. Shape Memory Alloys (SMAs) present unusual behaviour compared to more standard linear elastic materials. Indeed, they can accomodate large reversibe strain (pseudo-elasticity) or recover their shape, after being strained, by simple heating (shape memory effect). These behaviours are due to a displacive first order phase transformation called martensitic transformation. These features promote their use in many applications ranging from biomedical field to spatial domain. In the current work, we focus on the pseudoelastic behaviour. To this end, the thermomechanical constitituve law developped by Moumni and Zaki [1] is used. Firstly, the behaviour is reduced to a single degree of freedom. Secondly, inertial effect is considered and the forced oscillations of a device witnessing a pseudoelastic behaviour are studied. The analysis of the results through frequency-response curves and Poincaré maps reveals softening behaviour, jump phenomena, symmetry-breaking bifurcations and occurence of chaos. Results are in good agreement with those found in the literature [2] and using a different modelisation of the shape-memory effect.
Keywords: hysteresis loop, damping capacity, softening behaviour, chaotic solutions, symmetry breaking, Poincaré map.

1 Introduction

The interesting behaviour of shape memory alloys (SMA) is usually attributed to their ability to undergo a reversible solid - solid phase change between a parent phase called austenite and a product phase called martensite. The transition from austenite to martensite is accompanied by a loss of crystallographic symmetry, which produces entropy and heat. Austenite can usually transform into martensite when the SMA is mechanically stressed, the resulting transformation strain can then be recovered by unloading. This seemingly elastic yet dissipative behaviour is called *pseudoelasticity*. During a pseudoelastic transformation, a considerable amount of heat can be generated due to phase change, which can result in temperature variations that readily impact the behaviour of the SMA resulting in a strong thermomechanical coupling. This paper is devoted to the computation of the dynamic

response of a pseudoelastic device in isothermal condition. The behaviour of the device is derived from a full 3D model that has been exhaustively presented in [1]. It is recalled in section 2. The reduction to a one-dimensional system is exhibited in section 3 by assuming axial loading of a slender beam, resulting in a non-linear pseudoelastic spring characteristic. An added mass ensures inertia effect, and the oscillator model is completed with a dashpot and external harmonic forcing. Comparing with the model used in [2], [3] and [4], the originality of the current work is the use of a thermodynamic admissible 3-D law which allows studying vibrations of either continuous or discrete systems. The frequency-response of the pseudoelastic device is computed in the vicinity of its eigenfrequency corresponding to purely austenitic (small amplitude) motions. In the lines of the results presented in [2], a softening behaviour, characterized by a shift of the resonance frequency to lower frequencies, is found, resulting in jump phenomena. Moreover, symmetry-breaking bifurcations and onset of chaotic responses are detected for selected parameters values.

2 ZM model-3D version

The Zaki-Moumni (ZM) model for shape memory alloys is based on the of solid-solid phase change modelisation developed by Moumni [5] and was first introduced by Zaki and Moumni [1]. It was later extended to take into account cyclic SMA behaviour and training [6], tension-compression asymmetry [7] and irrecoverable plastic deformation of martensite [8]. The model is developed within the framework of Generalized Standard Materials with internal constraints ([9], [5]) in order to guarantee thermodynamic consistency. For the original ZM model, the thermodynamic potential is chosen as the Helmholtz free energy density taken as:

$$
\begin{aligned}
\mathcal{W} = (1-z) &\left[\frac{1}{2} \left(\boldsymbol{\epsilon}_\mathrm{A} \right) : \boldsymbol{S}_\mathrm{A}^{-1} : \left(\boldsymbol{\epsilon}_\mathrm{A} \right) \right] \\
&+ z \left[\frac{1}{2} \left(\boldsymbol{\epsilon}_\mathrm{M} - \boldsymbol{\epsilon}_\mathrm{ori} \right) : \boldsymbol{S}_\mathrm{M}^{-1} : \left(\boldsymbol{\epsilon}_\mathrm{M} - \boldsymbol{\epsilon}_\mathrm{ori} \right) + C(T) \right] \\
&+ G \frac{z^2}{2} + \frac{z}{2} \left[\alpha z + \beta \left(1 - z \right) \right] \left(\frac{2}{3} \boldsymbol{\epsilon}_\mathrm{ori} : \boldsymbol{\epsilon}_\mathrm{ori} \right)
\end{aligned}
\tag{1}
$$

In the above equation, $\boldsymbol{\epsilon}_\mathrm{A}$ and $\boldsymbol{\epsilon}_\mathrm{M}$ are the local strain tensors of austenite and martensite respectively, T is temperature, z is the volume fraction of martensite, and $\boldsymbol{\epsilon}_\mathrm{ori}$ is the orientation strain tensor. $\boldsymbol{S}_\mathrm{A}$ and $\boldsymbol{S}_\mathrm{M}$ are the compliance tensors of austenite and martensite respectively. ρ is the mass density, G, α, and β are material parameters that influences the shape of the superelastic hysteresis loop and the slopes of the stress-strain curve during phase change and martensite orientation. The parameter $C(T)$ is an energy density that depends on temperature as follows:

$$
C(T) = \xi(T - T^0) + \kappa,
\tag{2}
$$

where ξ and κ are material parameters. The state variables obey the following physical constraints :

- The macroscopic strain tensor $\boldsymbol{\epsilon}$ is an average over the REV (Representative Elementary Volume) of the strain within austenite and martensite phases. By construction, $\boldsymbol{\epsilon}$ is given by

$$(1 - z)\,\boldsymbol{\epsilon}_{\mathrm{A}} + z\boldsymbol{\epsilon}_{\mathrm{M}} - \boldsymbol{\epsilon} = 0, \tag{3}$$

- z is the volume fraction of martensite, restricted to the [0,1] interval,
- The equivalent orientation strain cannot exceed a maximum γ:

$$\gamma - \sqrt{\frac{2}{3}\boldsymbol{\epsilon}_{\mathrm{ori}} : \boldsymbol{\epsilon}_{\mathrm{ori}}} \geq 0. \tag{4}$$

The above constraints derive from the following potential:

$$W_{\mathrm{l}} = -\boldsymbol{\lambda} : [(1 - z)\,\boldsymbol{\epsilon}_{\mathrm{A}} + z\boldsymbol{\epsilon}_{\mathrm{M}} - \boldsymbol{\epsilon}] - \mu\left(\gamma - \sqrt{\frac{2}{3}\boldsymbol{\epsilon}_{\mathrm{ori}} : \boldsymbol{\epsilon}_{\mathrm{ori}}}\right) - \nu_1 z - \nu_2\,(1 - z)\,, \tag{5}$$

where the Lagrange multipliers ν_1, ν_2, and μ are such that

$$\begin{aligned} &\nu_1 \geq 0, \nu_1 z = 0, \\ &\nu_2 \geq 0, \nu_2\,(1 - z) = 0, \\ &\text{and } \mu \geq 0, \mu\left(\gamma - \sqrt{\frac{2}{3}\boldsymbol{\epsilon}_{\mathrm{ori}} : \boldsymbol{\epsilon}_{\mathrm{ori}}}\right) = 0. \end{aligned} \tag{6}$$

The sum of the Helmholtz energy density (1) and the potential W_{l} (5) gives the Lagrangian $\mathcal{L}$, which is then used to derive the state equations. With some algebra, the following stress-strain relation is obtained:

$$\boldsymbol{\sigma} = \boldsymbol{S}^{-1} : (\boldsymbol{\epsilon} - z\boldsymbol{\epsilon}_{\mathrm{ori}})\,, \tag{7}$$

where $\boldsymbol{S}$ is the equivalent compliance tensor of the material, given by

$$\boldsymbol{S} = (1 - z)\,\boldsymbol{S}_{\mathrm{A}} + z\boldsymbol{S}_{\mathrm{M}}. \tag{8}$$

The thermodynamic forces associated with z and $\boldsymbol{\epsilon}_{\mathrm{ori}}$ are taken as subgradients of a pseudo-potential of dissipation D defined as

$$D = [a\,(1 - z) + bz]\,|\dot{z}| + z^2 Y \sqrt{\frac{2}{3}\dot{\boldsymbol{\epsilon}}_{\mathrm{ori}} : \dot{\boldsymbol{\epsilon}}_{\mathrm{ori}}}, \tag{9}$$

where a, b are positive material parameters, and Y is a parameter linked to the orientation yield stress. This allows the definition of yield functions for phase change ($\mathcal{F}_{\mathrm{z}}^1$ and $\mathcal{F}_{\mathrm{z}}^2$) and for martensite orientation ($\mathcal{F}_{\mathrm{ori}}$). The evolutions of the state variables z and $\boldsymbol{\epsilon}_{\mathrm{ori}}$ are governed by the consistency

conditions associated with yield functions. If the orientation-finish stress is lower than the critical stress for forward phase change (*i.e.* if $\sigma_{\mathrm{rf}} < \sigma_{\mathrm{ms}}$), the model is such that the stress-induced martensite is completely oriented as soon as forward phase change begins.

In the next section, the ZM model will be reduced to 1D dimension in order to derive the dynamic response of a SMA device.

3   SMAs device-1D version

A single degree of freedom device can be considered by using a SMA beam with length l and cross-section area S. The SMA beam can be assimilated to a spring with nonlinear stiffness by studying relative displacement of its extremities. Figure 1 represents a sketch of the device, where a viscous structural damping $(\mathcal{C})$ is added to model internal losses that are not contained into the hysteresis loop. The mass $\mathcal{M}$ is subjected to external harmonic excitation of amplitude E_{max} and frequency ω as: $\mathcal{E}_e(t) = E_{max} \cos(\omega t)$. Assuming that in the direction $(\overrightarrow{x})$, $\sigma_{xx} = \left(\frac{F}{S}\right)$, $\varepsilon_{xx} = \left(\frac{X}{l}\right)$ and $\varepsilon_{ori,xx} = \left(\frac{X_{ori}}{l}\right)$, dimensioned model equations are summarized in table 1, where $\mathcal{K}(z)$ represents the nonlinear stiffnes. It is defined by: $\mathcal{K}(z) = \left(\frac{1-z}{\mathcal{K}_a} + \frac{z}{\mathcal{K}_m}\right)^{-1}$, where $\mathcal{K}_a = \left(\frac{E_a S}{l}\right)$ (respectively $\mathcal{K}_m = \left(\frac{E_m S}{l}\right)$) is the the stiffness in austenitic phase (resp. martensitic phase), related to their respective Young's modulus E_a and E_m. In the remainder, forward transformation means phase change from *austenitic* phase to *martensitic* one and reverse transformation in the inverse direction. Finally, X_{ori} is an internal displacement of the device due to detwinning process and is defined by $X_{ori} = X_{max} sgn\,(F)$, where $sgn(F)$ stands for the sign of F; a, b, G, α, β, ε_0, ξ, κ, θ_0 and Y are material parameters [1].

Motion equation :

$\mathcal{M}\ddot{X} + \mathcal{C}\dot{X} + F(X, z, X_{ori}) = \mathcal{E}_e(t)$

Behaviour equation :

$F(X, z, X_{ori}) = \mathcal{K}(z)\,(X - z.X_{ori})$

Thermodynamic force :

$\mathcal{A}_z = \frac{-1}{2E_a}\left(\frac{F}{S}\right)^2 + \frac{1}{2E_m}\left(\frac{F}{S}\right)^2 + \frac{1}{Sl}F.X_{ori} - C(T) - Gz - \left((\alpha - \beta)z + \frac{\beta}{2}\right)\left(\frac{X_{ori}}{l}\right)^2,$

Forward transformation criterion :

$\mathcal{F}_1^{cri} = \mathcal{A}_z - a\,(1 - z) - bz$

Reverse transformation criterion :

$\mathcal{F}_2^{cri} = -\mathcal{A}_z - a\,(1 - z) - bz$

Table 1. Dimensionalized equations
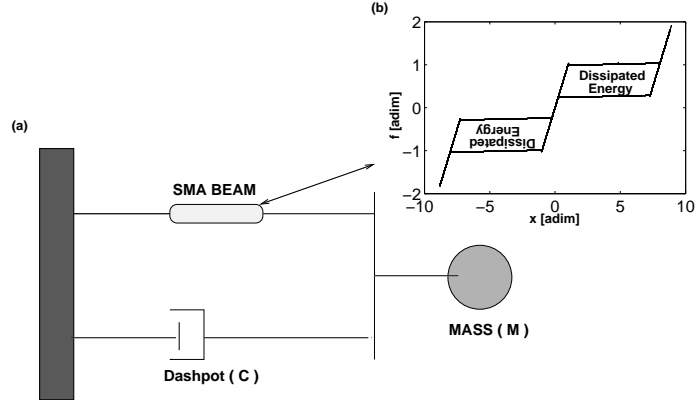
Fig. 1. (a) The pseudo-elastic device (b) Pseudo-elastic behaviour of the SMA beam

For calculations convenience, the following dimensionless equations are introduced : $\Omega = \frac{\omega}{\omega_n}, \tau = \omega_n t$, $x = \frac{X}{X_{ms}}, \gamma = \frac{E_{max}}{F_{ms}}, \zeta = \frac{C}{2\omega_n \mathcal{M}}$ and $f = \frac{F}{F_{ms}}$ where ω_n is the natural frequency of the device in its *austenitic* phase and is given by $\omega_n = \sqrt{\frac{\mathcal{K}_a}{\mathcal{M}}}$, X_{ms} and F_{ms} are respectively displacement and force tresholds of forward transformation. Assuming $\mathcal{K}_a = \mathcal{K}_m$, the dynamics of the systems is finally given by:

$$\begin{cases} \ddot{x} + 2\zeta\dot{x} + (x - z.x_{ori}) = \gamma \cos \Omega\tau & (10) \\ f(x, z, x_{ori}) = (x - z.x_{ori}) & (11) \end{cases}$$

A Newmark scheme for time integration of motion equation with parameters $\gamma_1 = \frac{1}{2}$ and $\beta_1 = \frac{1}{4}$ is used, where the internal Newton-Raphson iterations allows incremental fulfillement of the conditions provided by the criteria functions.

4 Results and discussion

In the remainder of the paper, the material parameters and the damping coefficient have been set to: a=17.920Mpa, b=17.920Mpa, $\varepsilon_0 = 0.112$, $\alpha = 1.4732Gpa$, $\beta = 1.4732Gpa$, $G = 26.88Mpa$, $\kappa = 8.68Mpa$, $\xi = 0.53114Mpa/^oC$, $T_0 = 233.3498K$, $A_f = 238.5945K$, $Y = 164Mpa$, $E_a = 50Gpa$, $E_m = 50Gpa$ and $\zeta = 0.05$. These values have been identified from the simulations shown in [2] in order to compare results. Frequency-response curves are obtained, for a given excitation frequency Ω, by numerical integration. The transient is removed and the maximal value of the displacement is recorded. Ω is then increased and decreased so as to obtain all stables branches of solutions. Figure 2 (a) shows the results obtained for increasing values of γ. For $\gamma = 0.1$, the response is linear, as no phase change is involved for that amplitude of response. For $\gamma = 0.2$ and $\gamma = 0.5$, the amplitude of the response exceeds 1: phase transformation occurs and the non-linear behaviour is characterized by a softening-type nonlinearity, as the resonance

frequency is seen to shift to lower values. Indeed, the equivalent stiffness of the pseudoelastic oscillator decreases. Saddle-node bifurcation points are then noted at points **A**, **B**,**C** and **D**, where jump phenomena are observed: when continuously varying the excitation frequency, the solution jumps to a stable solution to another one. For highest amplitude $\gamma = 0.8$, an additional branch of solutions is found between points **F** and **G**, it corresponds to cases where the phase transformation is completed ; the material becomes fully martensitic. The solution branch is bent to high frequencies as the stiffness increases from the transition plateaus to the purely martensitic case, with a volumic fraction z equal to 1. These results agree well with those in [2]. To go beyond, the amplitude $\gamma = 1.2$ is computed, results are shown in Fig. 2 (b). Before the resonance, for $\Omega \in [0, 0.5]$, a succession of erratic points are found, corresponding to the occurrence of superharmonic resonances of different orders. In order to get insight into the observed regimes for $\Omega \in [0, 0.5]$,
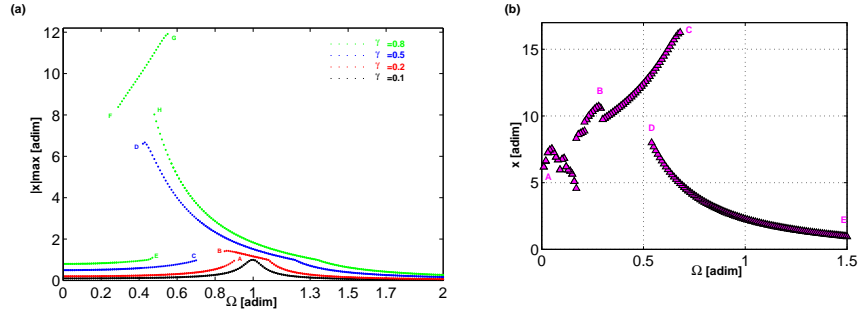

Fig. 2. (a)x_{max} vs. Ω at different γ, (b) x_{max} vs. Ω at $\gamma = 1.2$

Poincaré maps are computed by making a stroboscopy of the response at the excitation frequencies. Results are presented in Fig.3, they clearly show the presence of chaos for a narrow frequency band [0.22, 0.28]. By decreasing the excitation frequency, a period-doubling route to chaos is observed from point **D**. On the other hand, for $\Omega \in [0, 0.22]$, periodic solutions persist. The chaotic solutions at the beginning of their existence window, namely for $\Omega = 0.23$, are shown in Fig.4(a). The temporal solution shows that chaos is driven by the erratic behaviour of the enveloppe. Phase portrait reveals a fractal attractor. Interestingly, Fig.4(b) shows the emergence of even harmonics in the FFT of the displacement signal although the behaviour is symmetric. This shows that the bifurcation scenario when entering the chaotic window from low-frequencies is that of a symmetry-breaking bifurcation, as already observed in the Duffing oscillator [10].
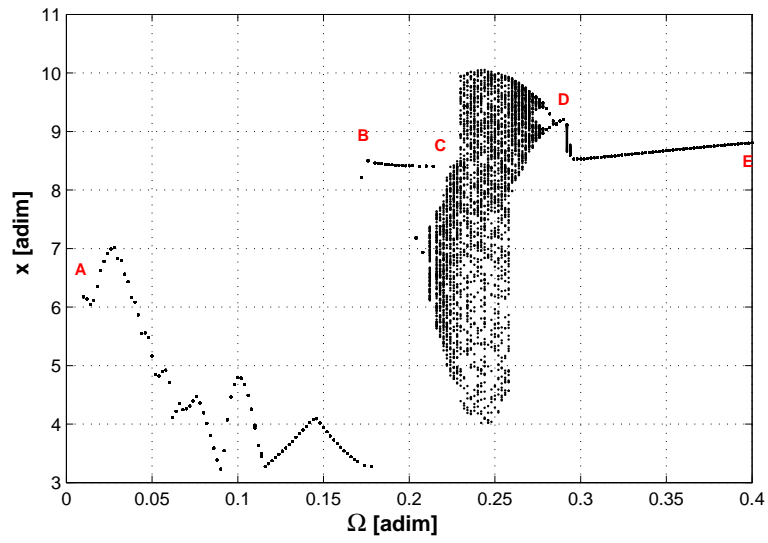
Fig. 3. Poincaré map at $\gamma = 1.2$
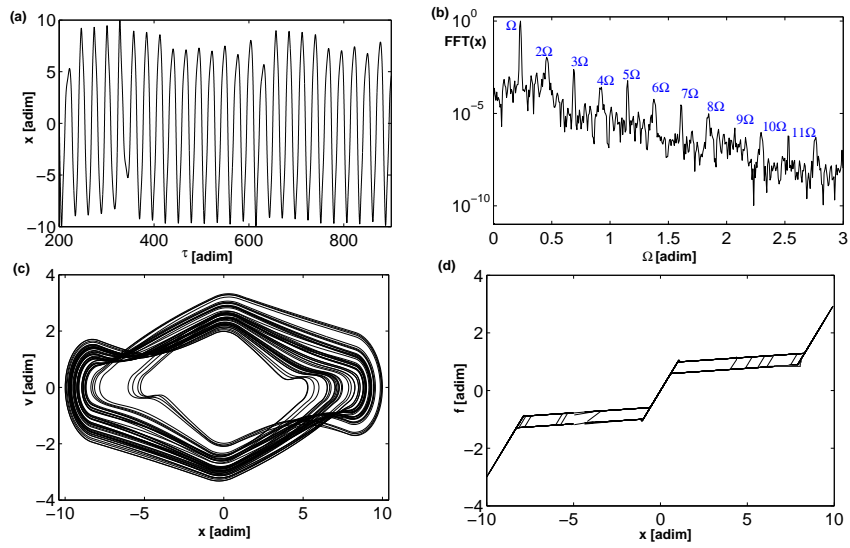
Fig. 4. (a) x vs. τ, (b) FFT(x) vs. Ω, (c) v vs. x and (d) f vs. x at $\gamma = 1.2$ and $\Omega = 0.23$:

5   Conclusion

The non-linear dynamic responses of pseudoelastic SMAs have been studied through reduction of a complete 3D model to a single degree-of-freedom oscillator. Results shows the emergence of chaotic solutions in the computed responses, for high values of the forcing amplitude. The chaotic region is delimited by a symmetry-breaking bifurcation and a period-doubling scenario.

References

1. Zaki W. and Moumni Z. A three-dimensional model of the thermomechanical behavior of shape memory alloys. *Journal of the Mechanics and Physics of Solids*, 55(11):2455–2490, 2007.
2. Lacarbonara W., Bernardini D., and Vestroni F. Nonlinear thermomechanical oscillations of shape-memory devices. *International Journal of Solids and Structures*, 41:1209–1234, 2004.
3. Bernardini D. and Vestroni F. Non-isothermal oscillations of pseudoelastic devices. *International Journal of Non-Linear Mechanics*, 38:1297–1313, 2003.
4. Bernardini D. and Rega G. The influence of model parameters and of the thermomechanical coupling on the behavior of shape memory devices. *International Journal of Non-Linear Mechanics*, 2009.
5. Moumni Z., Zaki W., and NGuyen Q.S. Theoretical and numerical modeling of solid-solid phase change : Application to the description of the thermomechanical behavior of shape memory alloys. *International Journal of Plasticity*, 24:614–645, 2008.
6. Zaki W. and Moumni Z. A 3d model of the cyclic thermomechanical behavior of shape memory alloys. *Journal of the Mechanics and Physics of Solids*, 55(11):2427–2454, 2007.
7. Zaki W. An approach to modeling tensile-compressive asymmetry for martensitic shape memory alloys. *Smart Materials and Structures*, 19 (2010) 025009 (7pp), 2010.
8. Zaki W., Zamfir S., and Moumni Z. An extension of the zm model for shape memory alloys accounting for plastic deformation. *Mechanics of Materials*, 42:266–274, 2010.
9. Moumni Z. Sur la modélisation du changement de phase solide : application aux maté- riaux à mémoire de forme et à endommagement fragile partiel. *Thèse de doctorat, Ecole Nationale des Ponts et Chaussées*, 1995.
10. Parlitz U. and Lauterborn W. Superstructure in the bifurcation set of the duffing equation. *Physics Letters A*, 107(8):351–355, 1985.